

# RSC Advances



This is an *Accepted Manuscript*, which has been through the Royal Society of Chemistry peer review process and has been accepted for publication.

*Accepted Manuscripts* are published online shortly after acceptance, before technical editing, formatting and proof reading. Using this free service, authors can make their results available to the community, in citable form, before we publish the edited article. This *Accepted Manuscript* will be replaced by the edited, formatted and paginated article as soon as this is available.

You can find more information about *Accepted Manuscripts* in the [Information for Authors](#).

Please note that technical editing may introduce minor changes to the text and/or graphics, which may alter content. The journal's standard [Terms & Conditions](#) and the [Ethical guidelines](#) still apply. In no event shall the Royal Society of Chemistry be held responsible for any errors or omissions in this *Accepted Manuscript* or any consequences arising from the use of any information it contains.

## Enhanced magneto-capacitance response in BaTiO<sub>3</sub>-ferrite composite systems

Sreenivasulu Pachari, Swadesh K. Pratihari, Bibhuti B. Nayak\*

Department of Ceramic Engineering National Institute of Technology Rourkela INDIA-769008

### Abstract

This research work focuses on the enhanced magneto-capacitance response in the composites of (1-X) BaTiO<sub>3</sub>: X (CoFe<sub>2</sub>O<sub>4</sub>/ ZnFe<sub>2</sub>O<sub>4</sub>/ Co<sub>0.5</sub>Zn<sub>0.5</sub>Fe<sub>2</sub>O<sub>4</sub>) (where X = 20, 30 and 40 wt %), prepared via conventional solid-state mixing route using auto-combustion derived powders. A new observation is the existence of two different types of morphologies such as plate-like (size was ~5 μm with a thickness ~1 μm) and fine agglomerated nearly spherical shape of tetragonal BaTiO<sub>3</sub> along with polyhedral morphology (size of ~0.5 to ~2.5 μm) of cubic ferrites in the prepared composite systems. Unidirectional or random orientation of plate-like morphology of BaTiO<sub>3</sub> in these composite systems depends on the percentage of ferrite phase. In addition to morphology effect, the magnetoresistance effect was analyzed using magneto-impedance study as a function of frequency as well as Cole-Cole plot. Magnetoresistance effect was found to be dependent on type and percentage of ferrites. The combined effects of phase morphology along with magnetoresistance and or magnetostriction led to enhance the magneto-capacitance response in these composites. The magnetocapacitance values were found to be in the range between -3 to -9, -0.5 to -7 and +1.5 to -1.5 for BaTiO<sub>3</sub>: CoFe<sub>2</sub>O<sub>4</sub>, BaTiO<sub>3</sub>: ZnFe<sub>2</sub>O<sub>4</sub> and BaTiO<sub>3</sub>: Co<sub>0.5</sub>Zn<sub>0.5</sub>Fe<sub>2</sub>O<sub>4</sub> composites, respectively depending on the percentage of ferrite phase.

**Keywords:** Solid state mixing; Magneto-dielectric; Composites; Magneto-capacitance; Ferrites, Barium titanate; Magnetoimpedance.

\*Corresponding address: bbnayak@nitrkl.ac.in, bibhutib@gmail.com (Bibhuti B. Nayak)

## Introduction

Magneto-dielectric composite materials are those which possess both magnetic and dielectric properties. Due to the stress mediated mechanical coupling between the dielectric [such as barium titanate ( $\text{BaTiO}_3$ )] and ferromagnetic (such as ferrites) phases, the magnetic properties can be controlled by an applied electric field, while the dielectric properties can be controlled by applying a magnetic field.<sup>1-9</sup> One of the important properties of magneto-dielectric composite system is magneto-capacitance response, which has potential applications in the field of sensors, actuators, and devices<sup>1,2,4,10-14</sup>. The magneto-capacitance response strongly depends on the magnetoresistance of grain or grain boundary, magnetostriction of ferrite phase as well as concentration of ferrite phase<sup>4,8,14</sup>. Also the distribution of ferroelectric ( $\text{BaTiO}_3$ ) and ferrimagnetic ferrites phases with different morphologies was reported to modify both magnetic and dielectric properties and hence magneto-capacitance of the composite system<sup>15</sup>. Different morphologies of  $\text{BaTiO}_3$  including spherical, cuboid, feather, pillars-like and polyhedral type ferrites have been explored in the  $\text{BaTiO}_3$ : ferrite composite system via various wet chemical synthesis methods such as molten-salt method, sol-gel method and hydrothermal-polymer assisted in-situ methods, respectively<sup>1,2,10, 16-23</sup>. Raidongia et.al.<sup>[15]</sup>, reported that magnetocapacitance increased from 1.7% to 4.5% by changing the morphology from core shell nano particles to core shell nanotubes. Change in the magnetocapacitance was also observed by Mandal et.al.<sup>[14]</sup>, in which  $\text{Co}_{0.65}\text{Zn}_{0.35}\text{Fe}_2\text{O}_4\text{-PbZr}_{0.52}\text{Ti}_{0.48}\text{O}_3$  magnetoelectric composites were prepared by sol-gel technique and had maximum capacitance change of 1.15% for 30 weight percent ferrite composite. Among different synthesis routes, solid-state mixing route was well established and lots of research has been carried out to prepare magneto-dielectric composites systems<sup>1,11,12,19-24</sup>. But, the formation of different morphologies of  $\text{BaTiO}_3$  or ferrite via solid-state mixing route is a challenge. So, combination of wet-chemical synthesis followed by solid-

state mixing may be another way to explore different types of morphologies of BaTiO<sub>3</sub> or ferrite in magneto-dielectric composite systems. Among the wet-chemical routes, auto-combustion has advantage of consuming less energy and time for developing oxide material.<sup>24</sup> Very few literatures are available for developing magneto-dielectric composite systems by solid-state mixing of auto-combustion derived powders. In this present work, three different types of ferrite were incorporated in the matrix of BaTiO<sub>3</sub> for the development of BaTiO<sub>3</sub>: ferrite composite materials via conventional solid-state mixing route using auto-combustion derived powders. Incorporation of different resistive ferrites may expect to modify the magnetocapacitance response of the magneto-dielectric composite materials. Thus, an attempt has been made to study the magneto-dielectric properties especially magneto-capacitance behavior of the composite with three different types of ferrites such as CoFe<sub>2</sub>O<sub>4</sub>, ZnFe<sub>2</sub>O<sub>4</sub> and Co<sub>0.5</sub>Zn<sub>0.5</sub>Fe<sub>2</sub>O<sub>4</sub>. The ferrite composition has been chosen based on the basis of their different electrical resistances<sup>25</sup>. Moreover, different morphology of BaTiO<sub>3</sub> along with different types of ferrite may enhance the magneto-capacitance response of these composite systems. So, the main objectives of this present work are (i) to explore different types of morphologies of BT or ferrite in BaTiO<sub>3</sub>: ferrite composite systems prepared via solid-state mixing of auto-combustion derived individual powders and (ii) to study the effect of ferrite type (CoFe<sub>2</sub>O<sub>4</sub>, ZnFe<sub>2</sub>O<sub>4</sub> and Co<sub>0.5</sub>Zn<sub>0.5</sub>Fe<sub>2</sub>O<sub>4</sub>) as well as its concentration on the microstructure and magneto-dielectric properties of BaTiO<sub>3</sub>: ferrite composite systems.

## Experimental

Raw materials such as barium nitrate [Ba (NO<sub>3</sub>)<sub>2</sub>], titanium nitrate [TiO (NO<sub>3</sub>)<sub>2</sub>], citric acid [C<sub>6</sub>H<sub>8</sub>O<sub>7</sub>], ammonium nitrate [NH<sub>4</sub>NO<sub>3</sub>] and EDTA [C<sub>10</sub>H<sub>16</sub>N<sub>2</sub>O<sub>8</sub>] were taken in the molar ratio of 1:1:1.5:12:0.1, respectively, for the synthesis of BaTiO<sub>3</sub> via auto-combustion route. Similarly, ferric nitrate nona-hydrate [Fe(NO<sub>3</sub>)<sub>3</sub>·9H<sub>2</sub>O], cobalt nitrate hexa hydrate [Co(NO<sub>3</sub>)<sub>2</sub>·6H<sub>2</sub>O], zinc

nitrate hexa- hydrate [ $\text{Zn}(\text{NO}_3)_2 \cdot 6\text{H}_2\text{O}$ ] and citric acid [ $\text{C}_6\text{H}_8\text{O}_7$ ] (3 moles citric acid was used for the mole of ferrite synthesized) were selected as raw materials in appropriate molar ratio for the combustion synthesis of ferrite compounds such as  $\text{CoFe}_2\text{O}_4$ ,  $\text{Co}_{0.5}\text{Zn}_{0.5}\text{Fe}_2\text{O}_4$  and  $\text{ZnFe}_2\text{O}_4$  via auto combustion method. The individual precursor solution for synthesizing  $\text{BaTiO}_3$  or ferrites was preceded by dissolving appropriate amount of the required reagents in distilled water and followed by adding ammonia to the precursor solution in order to achieve  $\text{pH} \sim 7$ . This solution was kept at  $80^\circ\text{C}$  under continuous stirring till a viscous gel was formed and this viscous gel proceeded by self-ignition followed by combustion. After combustion, the residue was collected and grounded in agate-mortar to form as-synthesized individual powders of  $\text{BaTiO}_3$  and ferrites. The combustion derived as-synthesized  $\text{BaTiO}_3$  and ferrites powders were calcined at  $1000^\circ\text{C}$  for 6h and  $900^\circ\text{C}$  for 4 h, respectively.

Further, the auto-combustion derived calcined ferrite ( $\text{CoFe}_2\text{O}_4/\text{ZnFe}_2\text{O}_4/\text{Co}_{0.5}\text{Zn}_{0.5}\text{Fe}_2\text{O}_4$ ) powders of 20, 30 and 40 wt % and appropriate amount of  $\text{BaTiO}_3$  were mixed properly in agate mortar using 3wt % PVA solution as binder. The dried mixed powders were compacted to pellets (average diameter and thickness of pellets are 10.70mm and 1.3mm) and sintered at  $1250^\circ\text{C}$  for 4 h based on the literature data<sup>26,27,28</sup>. Phase analysis using X-Ray diffractometer [model: Rigaku Ultima-IV, Japa], microstructure using Field Emission Scanning Electron Microscopy (FESEM) [model: NOVA Nano SEM/FEI 450], M-H loop measurement using M-H loop tracer [make: Magenta, India], dielectric measurements using LCR meter [model: HIOKI 3532-50 LCR Hitester] [Signal amplitude 100 mV, zero d.c. bias was used and data was produced using RC parallel circuit model], P-E loop measurement using P-E loop tracer [make: Marine India, Electronics] and magneto-capacitance [percentage  $\text{MC} = \{(\epsilon(\text{H}) - \epsilon(\text{H}=0)) / \epsilon(\text{H}=0)\} * 100$ , where  $\epsilon(\text{H})$  is permittivity at field and  $\epsilon(\text{H}=0)$  is permittivity without field] measurement (at 1KHz)

using both electromagnet [make: GMW magnet system, USA] and LCR meter were performed. In this paper, samples are specified with notation such as XBT\$Yferrite, where X stands for wt % of BaTiO<sub>3</sub> (BT) phase, \$ stands for solid-state mixing and Y stands for wt % of ferrite phase (CF/ZF/CZF).

## Results and discussion

Phase analysis of the sintered pellets of BT: ferrite composite systems were analyzed using X-ray diffraction pattern (XRD) and are shown in Fig. 1.

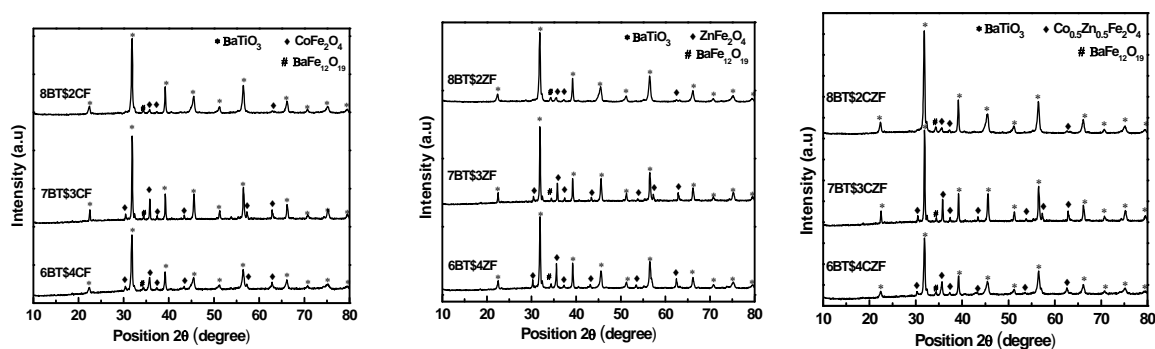


Fig. 1: X-ray diffraction patterns of solid-state derived BT: ferrite composite systems.

All the peaks were identified with either tetragonal BT (marked as \*) or cubic ferrite (marked as ♦) in the XRD pattern, as per the JCPDS data file (for BT: JCPDS file no: 75-2116 and for ferrite: JCPDS file no: 22-1086, 73-1963). In addition to these primary phases, minute amount of barium hexa-ferrite<sup>11,29</sup> (BaFe<sub>12</sub>O<sub>19</sub>) was also observed in all composites, due to diffusion of Fe<sup>2+</sup> or Fe<sup>3+</sup> ions in to Ti<sup>3+</sup> site.<sup>30</sup> It was also observed that the peak intensity of ferrite phase increases with increase in ferrite percentage in all composite systems<sup>31</sup>. The crystallite size of BT phase was found to be comparatively larger in size than the crystallite size of ferrite in the BT: ferrite composite systems. The crystallite size of BT phase was in the range between 26 nm to 34 nm, whereas, the crystallite size of ferrite was found to be in between 18 nm to 32 nm.

In order to study the microstructure, Field Emission Electron Microscopy (FESEM) was performed on BT: ferrite composites. Fig. 2 shows FESEM micrographs of BT: ferrites (CF/ZF/CZF) composite systems.

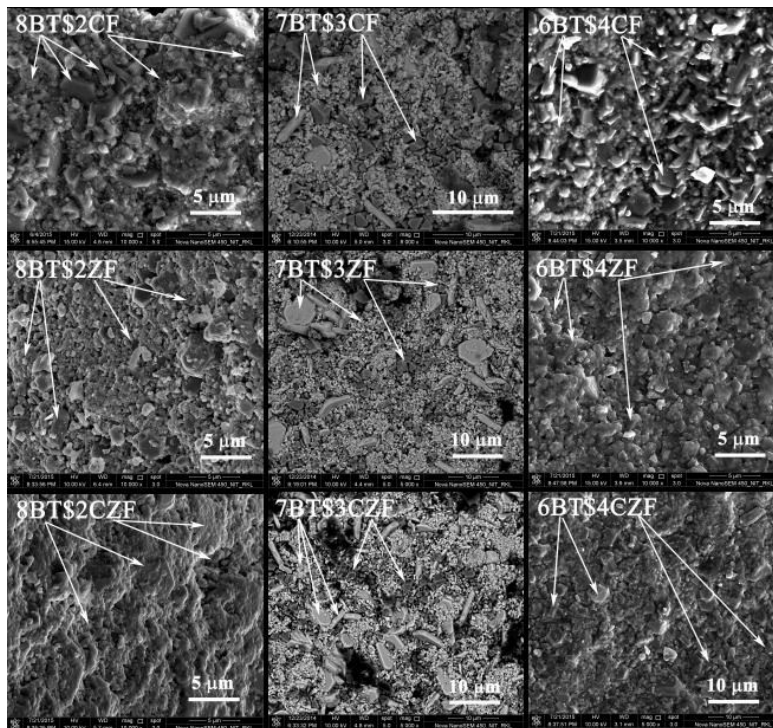


Fig. 2: FESEM micrographs of BT: ferrite composite systems. BT and ferrite phases were identified by arrow mark.

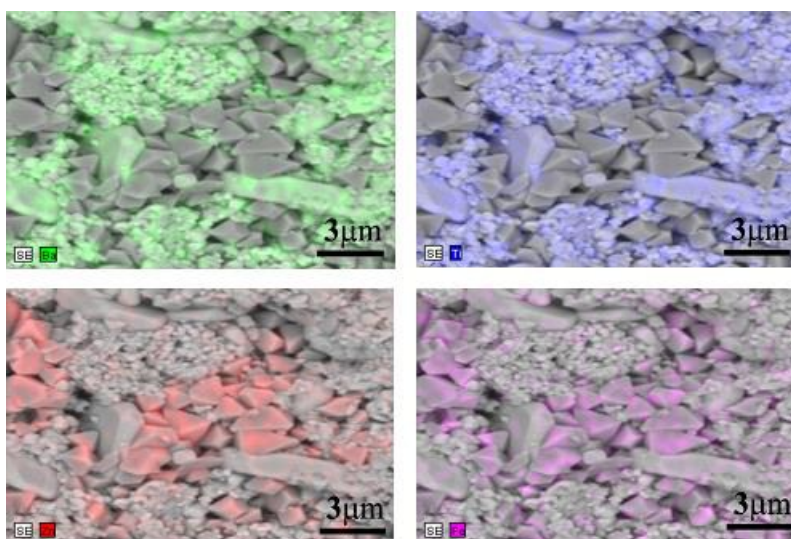


Fig. 3: Elemental mapping of 7BT\$3ZF composite. [Green: BT, Blue: Ti, Red: Zn and Pink: Fe]

Three different types of morphologies such as plate, polyhedral and agglomerated nearly spherical-like  $\text{BaTiO}_3$  phase were present in these composite systems. To further confirm the phases in the microstructure of BT: ferrite system, elemental mapping of typical 7BT\$3ZF composite was performed and shown in Fig. 3. From elemental analysis, it was clear that the plate and agglomerated nearly spherical-like morphologies belong to BT phase and the polyhedral-like morphology was ferrite phase. From FESEM micrographs in Fig. 2, it was confirmed that the particular plate-like BT phase was prominent in 7BT: 3 CF/ZF/CZF composite systems. In these particular composites, the plate-like BT phase was randomly oriented and the plates in vertical position resembling rod-like morphology. However, the plate-like BT phase was also present but orientated in one direction for other composite systems. From primary investigation of FESEM images, it would be presumable that the growth of polyhedral ferrite in 20 wt % ferrite based composites is lower and not sufficient enough to orient the plate-like morphology of BT phase and thus plate-like BT phase orient in one direction in 8BT: 2 CF/ZF/CZF composite systems. As the percentage of ferrite increases to 30 wt%, the polyhedral ferrite phase is prominent and its growth is sufficient to orient the plate-like BT phase in random way. Further increase of ferrite to 40 wt%, the growth of polyhedral ferrite phase increases and also partially covers the plate-like BT phase. So, in 6BT: 4 CF/ZF/CZF composite systems unidirectional plate like BT and polyhedral ferrite phases are with nearly same size and distribute undistinguished. The size of BT plates was  $\sim 5 \mu\text{m}$  with a thickness  $\sim 1 \mu\text{m}$ , whereas polyhedral ferrite was in between  $0.5\text{-}2.5 \mu\text{m}$ . Both BT and ferrite phases were well packed and seem to be highly dense. The density of these composites increases with ferrite content and varies in between 89-91%.

The variation of microstructure of BT: ferrite composite systems may lead to modify the dielectric and magnetic properties of these composites. So, one of the dielectric properties such as permittivity as a function of frequency of composite systems was analyzed at room temperature and are shown in Fig. 4.

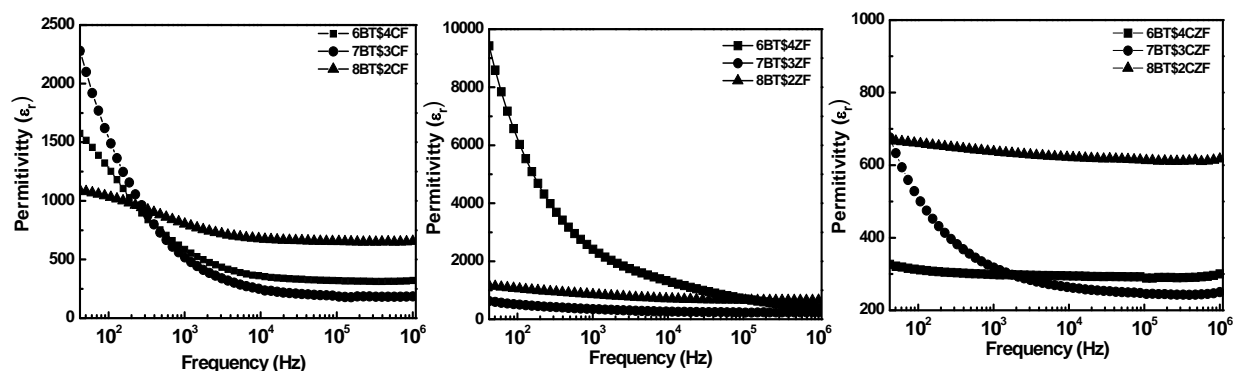


Fig. 4: Permittivity as a function of frequency for BT: ferrite composite systems.

Generally, for this type of composites, the permittivity decreases with frequency.<sup>29</sup> In this composite systems, it was observed that the permittivity was nearly independent with frequency for the composites having 20 wt % ferrite. However, the permittivity was dependent on frequency for the composites having 30 and 40 wt % ferrite. The nature of nearly independent or dependent permittivity with frequency for BT: ferrite composites may be depended on the concentration of BT phase and morphology along with distribution of BT and ferrite phase. In addition, sharply grown up permittivity at lower frequency for 30 wt% ferrite composites was due to Maxwell-Wagner interfacial polarization among randomly oriented plate like BT and polyhedral-like ferrite phases<sup>12,32</sup> or electrical charge depletion<sup>33</sup> between two phases. It was observed that composites having 30 wt % ferrite phase stood lower permittivity at higher frequency. However, the value of permittivity of the composite systems either increases or

decreases with increase in ferrite concentration due to involvement of Maxwell-Wagner affect, as three systems have different microstructures<sup>12,31, 32,34</sup>.

Dielectric loss is also one of the important parameter and thus was studied for the BT: ferrite composite systems at room temperature. Fig. 5 shows the loss ( $\tan \delta$ ) response with frequency for BT: ferrite composite systems. Dielectric loss is usually dependent on the dielectric phase and percentage of dielectric phase in the BT: ferrite composites. In addition loss is also dependent on the connectivity of the dielectric phase. Also, loss is inversely proportional to the dielectric percentage in the composites.<sup>35</sup> So, 20 wt % ferrite based BT: ferrite composites showing low loss as compared 30 and 40 wt % ferrite based composites. However, maximum loss was varies in between 0.83 to 1.37 in these composite systems. It was observed that the loss decreases with frequency having a hump type response prominent in cobalt and zinc ferrite based composite systems. This response in the composite can be attributed to the resonance of applied frequency with the hopping mechanism between  $\text{Fe}^{2+}$  and  $\text{Fe}^{3+}$  ions<sup>29</sup>.

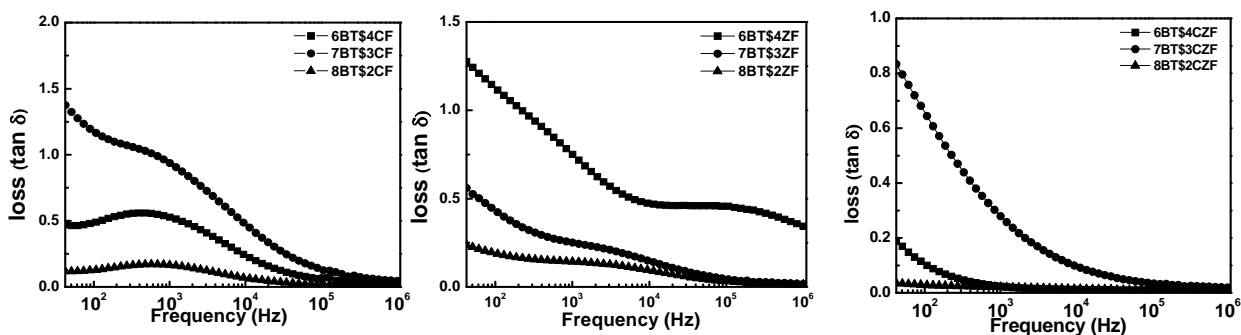


Fig.5: Dielectric loss as a function of frequency for BT: ferrite composite systems.

Polarization responses as a function of electric field of these composites are shown in Fig. 6. It was observed that the responses of PE loop in the BT: ferrite composites deviated from the ideal ferroelectric loop due to the individual phase morphologies as well as connection of BT phase in

the composite systems. The particular 30 or 40 wt % ferrite based composite systems appear in oval shape characteristics of a lossy capacitor due to field discharge by conductive ferrite phase.<sup>30,36</sup> However, 20 wt % ferrite based BT: ferrite composite systems shows near ferroelectric type behavior. Polarization (at maximum field) and coercivity of all composites are given in Table 1. The polarization of these composites varies in between 1.2 to 10.8  $\mu\text{C}/\text{cm}^2$  and coercivity varies in between 4 to 16 kV/cm depending on the ferrite type and percentage.

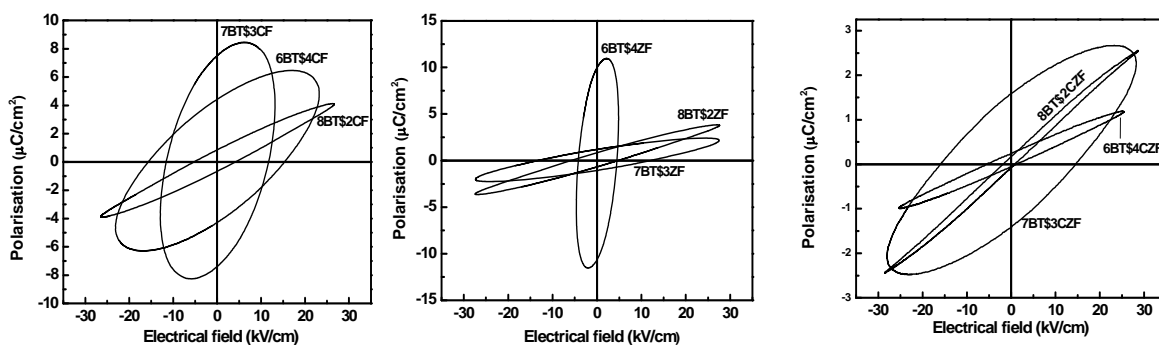


Fig. 6: polarization as function of electric field for BT: ferrite composite systems.

Similarly, magnetization as a function of magnetic field of BT: ferrite based composite systems was analyzed. Magnetization and coercivity data of BT: ferrite composite systems are given in Table: 1. M-H loop of all composites are look alike. However, the typical M-H loop of 30wt% ferrite composites are shown in fig: 7.

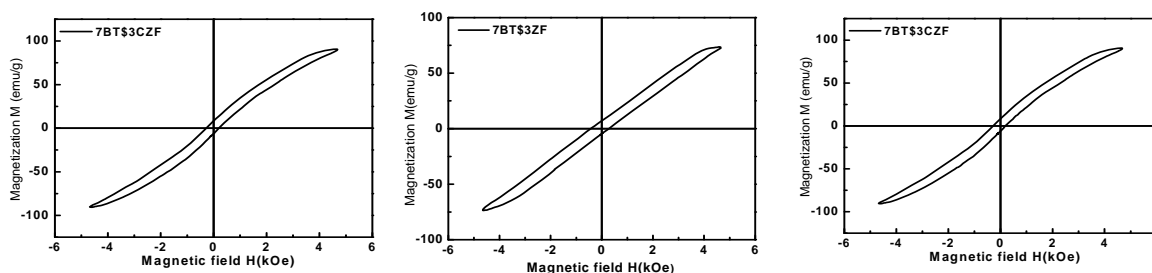


Fig. 7: M-H loop of 30 wt % ferrite based BT: ferrite composite systems.

It was observed that BT: CF and BT: CZF composites are ferromagnetic in nature due to the magnetic characteristics of CF or CZF. However, the presence of hard magnetic phase of BaFe<sub>12</sub>O<sub>19</sub> in the BT: ZF composites led to behave as ferromagnetic. Also, all these composites are ferromagnetic with non-saturating in nature due to the presence of different morphologies of BT phase, which act as a pinning center.<sup>14</sup> The pinning effect clearly indicates the strong mechanical interaction between the magnetic and non-magnetic phase<sup>14</sup>. From Table 1, it was observed that the magnetization (at 4.2 KOe) of the composites decreases with the increase in BT addition,<sup>13,34,37,38</sup> due to the reduced magnetic moments per unit volume.<sup>30</sup> Coercivity of the BT: ferrite composite systems depend on the ferrite concentration as well as the microstructure. In these composite systems, the coercivity varies in between 175 Oe to 325 Oe. However, the 30 wt% ferrite based composites have higher coercivity than other ferrite based composites due to pinning effect from plate-like morphologies of BT.

Table: 1: Coercivity ( $E_c$ ), polarization (P) (at maximum field), Coercivity ( $H_c$ ) and magnetization (M) of BT: ferrite composite systems.

Composites	Coercivity $E_c$ (kV/cm)	Polarization $P$ ( $\mu\text{C}/\text{cm}^2$ )	Coercivity $H_c$ (kOe)	Magnetization at 4 KOe (emu/g)
6BT\$4CF	16	6.49	0.305	91.74
7BT\$3CF	11.5	8.4	0.325	89.85
8BT\$2CF	5	4.4	0.262	69.56
6BT\$4ZF	4	10.8	0.309	73
7BT\$3ZF	13	2.3	0.315	65
8BT\$2ZF	5	3.77	0.291	64
6BT\$4CZF	5.6	1.2	0.175	90.81
7BT\$3CZF	16	2.6	0.203	84
8BT\$2CZF	1.7	2.54	0.184	70

Generally, magneto-capacitance response in the BT: ferrite based composites originates from the mechanical coupling between ferromagnetic and ferroelectric phases present in the

composites. Extrinsic parameters like magnetic/ferroelectric percentage and microstructure plays a significant role for enhancement of magneto-capacitance response<sup>15</sup>. In the present study, the variation in microstructure of BT: ferrite composite systems motivated to explore the magneto-capacitance response. So, in these composite systems, percentage change in magneto-capacitance response as a function of magnetic field was measured and shown in Fig.8. It was observed that the magneto-capacitance increases with increase in magnetic field and saturate at  $\sim 2$  K Oe. Both cobalt and zinc ferrite based composites followed the trend of increasing magneto-capacitance response with increase in percentage of ferrite. In addition, both cobalt and zinc ferrite based composites show negative magneto-capacitance response. However, cobalt-zinc ferrite based composite shows both negative (for 30 wt % ferrite) and positive (for 20 and 40 wt % ferrite) magneto-capacitance response.

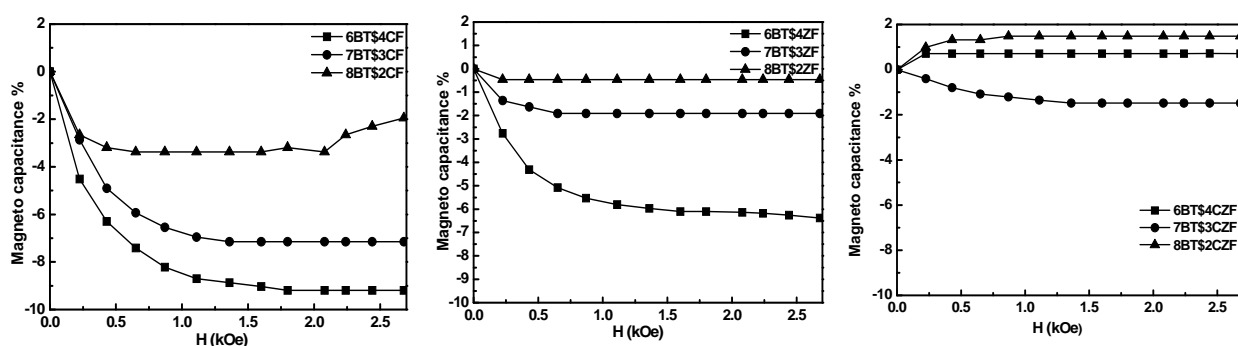


Fig. 8: Magneto-capacitance as function of magnetic field for BT: ferrite composite systems.

To explore further, magnetoimpedance  $[MI=(Z'(H)-Z'(O))/Z'(O)]$  values (at magnetic field of 2.68 kOe) as a function of frequency of these composite systems were determined and shown in Fig. 9. Also for better comparison, magneto-capacitance as a function of frequency of these BT: ferrite composite systems are presented in Fig. 10. By considering BT: CF composites, the magnetoimpedance behavior was found to be frequency dependent for all compositions.

However, 7BT\$3CF composite have nearly independent of frequency at lower frequency range (i.e. 42Hz to ~1kHz). Also, the relaxation behavior was clearly seen in the cobalt ferrite based compositions particularly for 20 and 40 wt % ferrite based composites by observing peaks at 100 Hz and also at 1M Hz. While, analyzing magnetocapacitance response of cobalt ferrite based composites in Fig. 10 at lower frequency range, it was revealed that the magnetocapacitance response was mainly due to involvement of magneto-resistance for particularly 20 and 40 wt % cobalt-ferrite based composites, whereas, the magnetocapacitance response in 30 wt % cobalt ferrite composite was due to the contribution of magnetostriction of CF phase in BT matrix. Also at lower frequency, 6BT\$4CF composite was higher value impedance, whereas, 8BT\$2CF composite shows lower impedance. Comparing with Fig. 10, the magneto-capacitance value was higher for 6BT\$4CF composite and lower for 8BT\$2CF composite. This indicates that the magnetoimpedance and magnetocapacitance are inverse with each other at lower frequency range. However, at higher frequency, the magnetoimpedance was found to be frequency dependent for BT: cobalt ferrite composite systems. But, magnetocapacitance behavior decreases and also frequency independent towards higher frequency. This suggests that the frequency independent magnetocapacitance behavior is due to insufficient time for charge carriers to respond to the applied field. Similarly, decreasing magneto-capacitance towards higher frequency is due to cancellation of magnetoresistance and M-W affect <sup>9</sup>. The above discussion was also applicable for BT: ZF and BT: CZF composite systems. In 30 and 40 wt % ferrite based BT: ZF and BT: CZF composite systems have nearly frequency independent magnetoimpedance response both at lower frequency as well as higher frequency range. However, 20 wt % ferrite based BT: ZF and BT: CZF composite systems have frequency dependent magnetoimpedance behavior having peak at ~ 1 kHz. Comparison Fig. 9 and Fig. 10 for BT: ZF and BT: CZF

composites having 30 and 40 wt % ferrites show frequency independent magneto-capacitance response which suggest that the magnetocapacitance originates from magnetostriction of ferrite phase. However, even small response of magnetocapacitance for 20 wt % ferrite based BT: ZF and BT: CZF composites have maximum contribution from magnetoresistance affect.

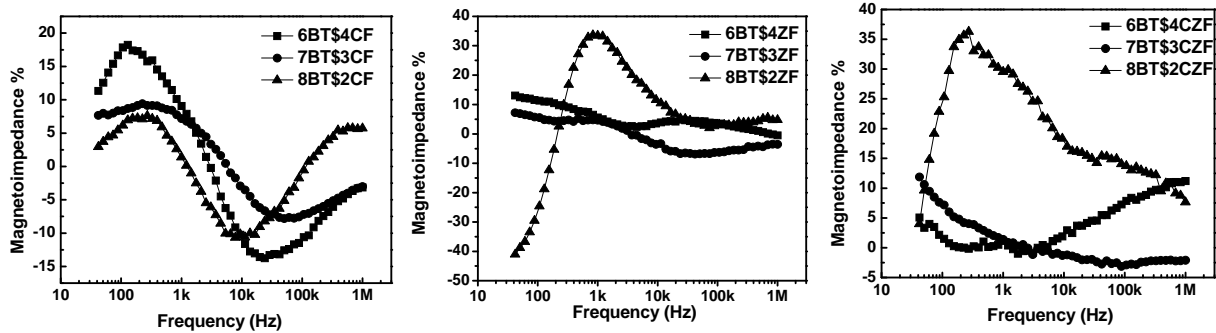


Fig. 9: Magneto-impedance as function of frequency for BT: ferrite composite systems.

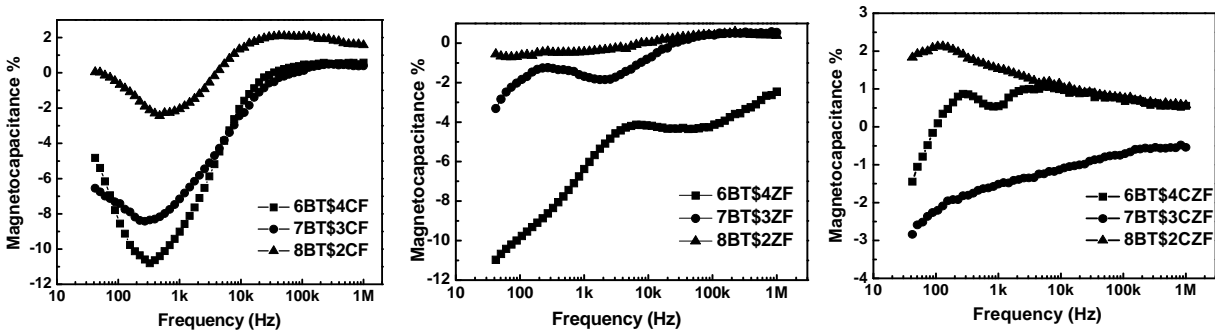


Fig. 10: Magneto-capacitance as function of frequency for BT: ferrite composite systems.

Further to support the origin of magnetocapacitance response in the present composite system, Cole-Cole graph was plotted for all composite systems without and with magnetic field (at 2.68 kOe) and is shown in Fig. 11. In case of BT: CF composite systems all compositions show a change in resistance with application of magnetic field except for the composite 7BT\$3CF. It further suggests that the magnetocapacitance behavior of the particular 7BT\$3CF composites originates from magnetostriction of CF phase. Whereas, the magneto-capacitance

behavior of both 8BT\$2CF and 6BT\$4CF composite are due to magnetoresistance affect. A small change in resistance was observed in both 30 and 40 wt % ferrite based composites of BT: ZF and BT: CZF, whereas, a quite large change in resistance with application of magnetic field was observed in the particular 20 wt % Zn- and Co-Zn ferrite based composite systems. This further support that the magnetocapacitance behavior of 30 and 40 wt % ferrite based BT: ZF and BT: CZF composite systems are mainly due to magnetostriction, whereas, magnetocapacitance behavior of 20 wt % ferrite based BT: ZF and BT: CZF composite systems are due to magnetoresistance.

Further, in order to understand the grain and grain boundary resistance, cole-cole graph was fitted with an equivalent circuit of  $R(Q_1R_1)(Q_2R_2)$  with the experimental data. It was found that for 30 and 40 wt % ferrite based BT: CF, BT: ZF and BT: CZF composite, the grain boundary resistance and capacitance remains nearly constant without and with application of magnetic field. However, for 20 wt % ferrite based composites, the grain boundary resistance and capacitance increases with the application of magnetic field. Hence, the samples with 20 % ferrite phase show a wide deviation of impedance in cole-cole plot.

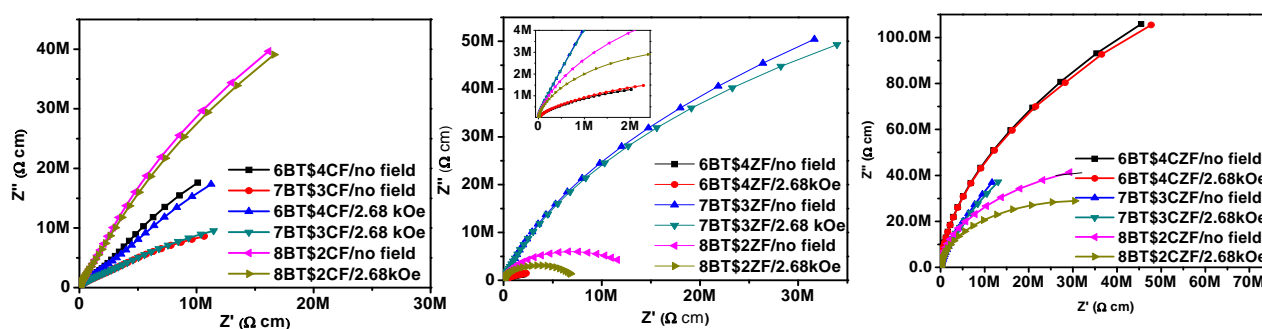


Fig. 11: Cole-Cole plots of BT: ferrite composite systems without and with magnetic field.

The origin of magneto-capacitance behavior in the present BT: ferrite composite systems can be explained in different ways: first, induced strain in the magnetic material due to applied

magnetic field can modify the magneto-capacitance of the composite by mechanical coupling<sup>14</sup>. Second, according to the Catalan,<sup>33</sup> the interfacial polarization effect in magneto-dielectric composite systems can also give magneto-capacitance response based on the resistance of the conducting grain or grain boundary with application of magnetic field. In addition, the microstructure or morphology of BT/ferrite phase may also effect the magneto-capacitance response that depend on the interfacial interaction between the dielectric and magnetic phases present in the composite.<sup>3,4,14,38</sup>

The positive or negative nature of magnetocapacitance in the present BT: ferrite composite systems strongly depend on the magnetostriction of ferrite phase, magnetoresistance of grain or grain boundary as well as morphology of BT phase. It was suggested that the negative magnetostriction of zinc ferrite led to show negative magnetocapacitance<sup>3,8</sup> in zinc-ferrite based composite system. However, negative magnetostriction of cobalt-zinc ferrite led to show positive magnetocapacitance in cobalt-zinc-ferrite based composite system<sup>14</sup>. But, the negative magnetostriction of cobalt ferrite led to show positive or negative magnetocapacitance in cobalt-ferrite based composite systems<sup>1,10,15,38</sup>. So, it is difficult to narrow down the link between sign of magnetostriction and magnetocapacitance in the magneto-dielectric composite system, however, the collected data is given in Table 2. In addition, core-dominated magnetoresistance and interface-dominated magnetoresistance give positive and negative magneto-capacitance, respectively<sup>33</sup>. Also, in the present system, it was found that the magnetoresistance or magnetostriction induced magnetocapacitance strongly depends on the composition of ferrite phase. The negative response of magneto-capacitance in both cobalt and zinc ferrite based composite systems was due to strong interaction between plate-like morphology of BT and polyhedral ferrite phase at the interface. Similar observation was also observed in most of the literatures and are well discussed based on the interfacial mechanical interaction or interface dominated magneto-resistance between the dielectric and magnetic phases<sup>33,38,3</sup>. However, both

positive and negative magneto-capacitance response in BT: CZF composites are due to the involvement of magnetoresistance or magnetostriction along with microstructural effect in which randomly oriented plate-like morphology of BT modifies the magneto-capacitance response. The values of magneto-capacitance in these composite systems are found to be enhanced, when compared with the literature data as given in Table 3.

Table 2: Sign of magnetostriction and direction of magnetocapacitance in the magneto-dielectric composite system collected from the literatures.

Sl. no	Composite system	Magnetocapacitance direction	Proposed sign of magnetostriction	[ref]
1	$\text{Co}_{0.65}\text{Zn}_{0.35}\text{Fe}_2\text{O}_4$ - $\text{PbZr}_{0.52}\text{Ti}_{0.48}\text{O}_3$	Positive	negative	[4],[14]
2	$\text{BaTiO}_3$ - $\text{ZnFe}_2\text{O}_4$	negative	negative	[4],[8]
3	$[\text{Ba}(\text{Sn}_{0.3}\text{Ti}_{0.7})\text{O}_3]_{0.8}$ - $[\text{CoFe}_2\text{O}_4]_{0.2}$	positive	negative	[1]
4	$\text{BaTiO}_3$ - $\text{CoFe}_2\text{O}_4$	negative	negative	[15]

Table 3: Maximum magnetocapacitance (%) values were collected from literature data and compare with the present system.

Sl.No	Composite system	Magnetocapacitance %	Composite type	[ref]
1	$\text{BaTiO}_3$ - $\text{CoFe}_2\text{O}_4$	-4.5 at 2.1 Tesla	Core and shell Bulk composites	[15]
2	$(\text{X})\text{Co}_{0.65}\text{Zn}_{0.35}\text{Fe}_2\text{O}_4$ -(1-X) $\text{PbZr}_{0.52}\text{Ti}_{0.48}\text{O}_3$	~1.1 at 7 tesla for X=0.3	Particulate Bulk composites	[14]
3	$\text{BaTiO}_3$ - $\text{ZnFe}_2\text{O}_4$	~-0.75 at 4 Tesla	Thin films	[5]
4	$\text{BaTiO}_3$ - $\text{CoFe}_2\text{O}_3$	2.5 at 75 kOe	Thin films	[6]
5	$(\text{X})\text{BaTiO}_3$ -(1-X) $\text{CoFe}_2\text{O}_3$	7.5 at 1.3 kOe for X=0.5	Particulate bulk composites	[7]
6	$\text{BaTiO}_3$ - $\text{ZnFe}_2\text{O}_3$	~-1.3 at 10 kOe	Core and shell bulk composites	[8]
7	$\text{BaTiO}_3$ - $\text{CoFe}_2\text{O}_3$	~3.8 at 7 kOe	Core and shell bulk composites	[9]
8	$(1-\text{X})\text{BaTiO}_3$ - $\text{XCoFe}_2\text{O}_4$	-3.9 at $4.5 \times 10^5$ A. $\text{m}^{-1}$	Particulate bulk composites	[38]
Present system	$(\text{X})\text{BaTiO}_3$ -(1-X) $\text{CoFe}_2\text{O}_3$	-9 at 2.68 kOe for X=0.6	Particulate bulk composites	
	$(\text{X})\text{BaTiO}_3$ -(1-X) $\text{Co}_{0.5}\text{Zn}_{0.5}\text{Fe}_2\text{O}_3$	-1.5 at 2.68 kOe for X=0.8 1.5 at 2.68 kOe for X=0.7		
	$(\text{X})\text{BaTiO}_3$ - $\text{ZnFe}_2\text{O}_3$	-7 at 2.68 kOe for X=0.6		

## Conclusions

Composite of BT: CF, BT: ZF and BT: CZF having 20, 30 and 40 wt % ferrite were successfully prepared via conventional solid-state mixing route using auto-combustion derived powders. The composite microstructure consists of plate-like (prominent in 7BT: 3 CF/ZF/CZF composite systems) as well as agglomerated spherical-like morphologies of BT and polyhedral-like morphology of ferrites. Frequency dependence dielectric behavior in these composites was well explained from the consideration of microstructural features such as distribution of phases, their amount and characteristics. Field discharge by conductive ferrite phase was found to be responsible for lossy behavior observed in PE loop. The pinning of BT phase in these composite systems shows non-saturating behavior of MH characteristics. The origin of magnetocapacitance response in these composite systems was well-correlated using magnetoimpedance against frequency and Cole-Cole graph. It was found that magneto-capacitance response of 7BT\$3CF, 7BT\$3ZF, 7BT\$3CZF, 6BT\$4ZF and 6BT\$4CZF composite arises due to magnetostriction of ferrite phase. However, the magnetocapacitance response of 8BT\$2CF, 6BT\$4CF, 8BT\$2ZF and 8BT\$2CZF composite was due to contribution of magneto-resistance. Involvement of either magnetoresistance and or magnetostriction along with morphology of BT phase in BT: ferrite composite systems have a role to tune as well as enhance the magneto-capacitance response in either positive or negative way depending on the percentage of ferrite phase.

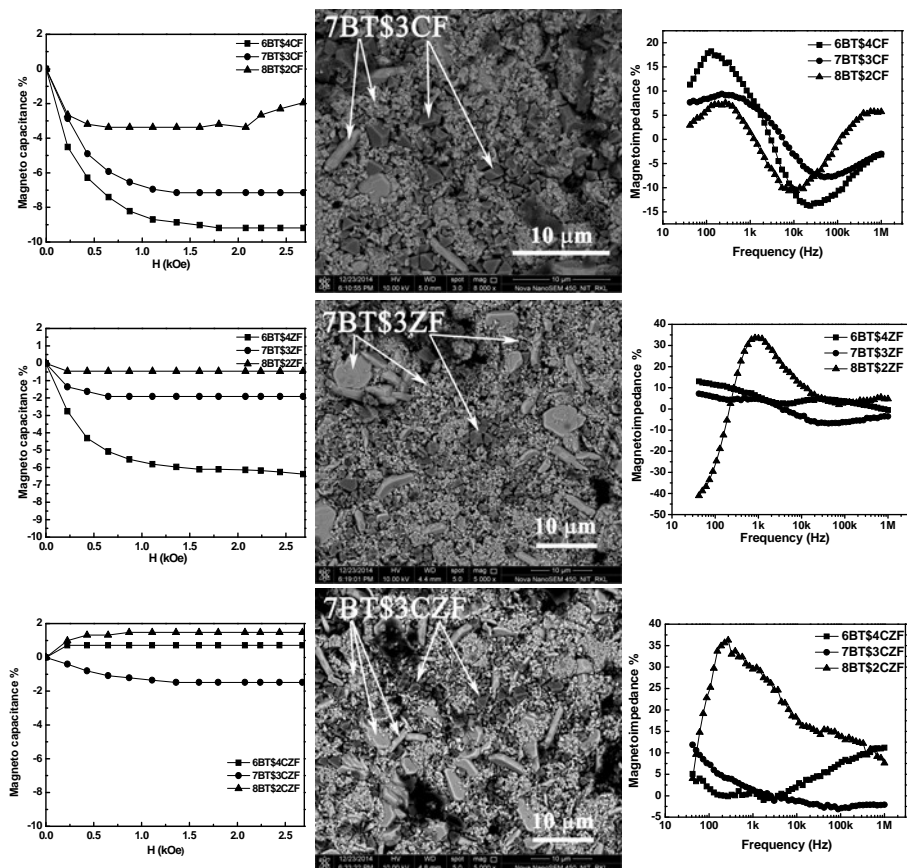
## References

1. M. N. Ul-Haq, T. Yunus, A. Mumtaz, V.V. Shvartsman and D. C. Lupascu, *J. Alloys Compd*, 2015, **640**, 462-467.
2. M. Stingaciu, P.G. Reuvekamp, C.-W. Tai, R. K. Kremer and M. Johnsson, *J. Mater. Chem. C*, 2014, **2**, 325-330.
3. K. C. Verma, S. K. Tripathy and R. K. Kotnala, *RSC Adv.*, 2014, **4**, 60234-60242.
4. G. Srinivasan, E. T. Rasmussen, and R. Hayes, *Phys. Rev. B.*, 2003, **67**, 014418.
5. M. Lorenz, M. Ziese, G. Wagner, J. Lenzner, C. Kranert, K. Brachwitz, H. Hochmuth, P. Esquinazi and M. Grundmann, *CrystEngComm*, 2012, **14**, 6477-6486
6. I. Fina, N. Dix, L. Fàbrega, F. Sánchez and J. Fontcuberta, *Thin Solid Films*, 2010, **518**, 4634-4636.
7. M. Rafique, S. Q. Hassan, M.S.Awanb and S. Manzoor, *Ceram. Int.*, 2013, **39**, S213-S216.
8. S. Singh, N. Kumar, R. Bhargava, M. Sahni, K. Sung and J.H. Jung, *J. Alloys Compd*, 2014, **587**, 437-441.
9. M. M. Selvi, P. Manimuthu, K. S. Kumar and C. Venkateswaran, *J. Magn. Magn. Mater.*, 2014, **369**, 155-161.
10. Y.Q. Dai, J.M. Dai, X.W. Tang, K.J. Zhang, X.B. Zhu, J. Yang and Y.P. Sun, *J. Alloys Compd*, 2014, **587** 681-687.
11. L. Curecheriu, P. Postolache, V. Buscaglia, N. Horchidan, M. Alexe and L. Mitoseriu, *Phase Transitions.*, 2013, **86(7)**, 670-680
12. A. Testino, L. Mitoseriu, V. Buscaglia, M.T. Buscaglia, I. Pallecchi A.S. Albuquerque, V. Calzona, D. Marr'e, A.S. Siri and P. Nanni, *J. Eur. Ceram. Soc.*, 2006, **26**, 3031-3036.
13. S. Agarwal, O.F.Caltun and K.Sreenivas, *Solid State Commun.*, 2012, **152**, 1951-1955.
14. P.R. Mandal and T.K. Nath, *J. Alloys Compd.*, 2014, **599**, 71-77.
15. K. Raidongia, A. Nag, A. Sundaresan and C. N. R. Rao, *Appl. Phys. Lett.*, 2010, **97**, 062904-3
16. D. Zhou, G. Jian, Y. Zheng, S. Gong and F. Shi, *Appl. Surf. Sci.*, 2011, **257**, 7621-7626.
17. L. Zhang, J. Zhai, W. Mo and X. Yao, *Solid State Sci.*, 2011, **13**, 321-325.
18. L. Zhang, J. Zhai, W. Mo and X. Yao, *Solid State Sci.*, 2010, **12**, 509-514.
19. I. Kagomiya, Y. Hayashi, K. Kakimoto and K. Kobayashi, *J. Magn. Magn. Mater.*, 2012, **324**, 2368-2372.

20. L. Zhang, J. Zhai, W. Mo and X. Yao, *Mater. Chem. Phys.*, 2009, **118**, 208-212.
21. H. Yang, G. Zhang, Y. Lin and F. Wang, *Mater. Lett.*, 2015, **157**, 99-102.
22. J. Nie, G. Xua, Y. Yangb and C. Cheng, *Mater. Chem. Phys.*, 2009, **115**, 400-403.
23. Y. Deng, J. Zhou, DiWuc, Y. Du, M. Zhang, D. Wang, H. Yu, S. Tang and Y. Du, *Chem. Phys. Lett.*, 2010, **496**, 301-305.
24. S. H. Xiao, W. F. Jiang, L. Y. Li and X. J. Li, *Mater. Chem. Phys.*, 2007, **106**, 82-87.
25. C. Heck, *Magnetic Materials and Their Applications*, Butterworths, London, 1974.
26. V corral-flores, D Bueno-Baques, D Carrilo-Flores, JA Matutes-Aquino, *J Appl Phys*, 2006, **99(8)**, 08J5031-3.
27. G.V. Duong, R. Groessinger, R.S Tirtelli, *IEEE Trans Magn*, 2006, **42(10)**, 3611-3613.
28. G.V. Duong, R. Groessinger, R.S Tirtelli, *J Magn Magn Mater*, 2007, **310(2)**, e361-3
29. H. Zhenga, W.J. Wenga, G.R. Hana and P.Y. Du, *Ceram. Int.*, 2015 **41**, 1511-1519.
30. A. khamkongkao, P. Jantaratana, C. Sirisathitkul, T. yamwong and S. Maensiri, *Trans. Nonferrous Met. Soc. China.*, 2011, **21**, 2438-2442.
31. Z. Yu and C. Ang, *J. Appl. Phys.*, 2002, **91(2)**, 794-797.
32. H. Yang, H. Wang, L. Hea and X. Yaoa, *Mater. Chem. Phys.*, 2012, **134**, 777-782.
33. G. Catalana, *Appl. Phys. Lett.*, 2006, **88**, 102902-3
34. H. Zheng, L. Li, Z. Xu, W. Weng, G. Han, N. Ma, and P. Du, *J. Appl. Phys*, 2013, **113**, 044101-8
35. R. Zhang, C. Deng, L. Ren, Z. Li and J. Zhou, *Mater. Res. Bull.*, 2013, **48**, 4100-4104.
36. M. Ghidini, F. Maccherozzi, X. Moya, L.C. Phillips, W. Yan, J. Soussi, N. Métallier, M.E. Vickers, N.-J. Steinke, R. Mansell, C.H.W. Barnes, S.S. Dhesi, N.D. Mathur, *Adv. Mater.* 2015, **27**, 1460–1465.
37. L. Mitoseriu, I. Pallecchi, V. Buscaglia, A. Testino, C.E. Ciomaga and A. Stancu, *J. Magn. Magn. Mater.*, 2007 **316**, e603-e606.
38. Y. Sen, J. Sun, L. Li, Y. Yao, C. Zhou, R. Su and Y. Yang, *J. Mater. Chem.C*, 2014, **2**, 2545-2551.

## Table of Content

### Graphical Abstract



#### Text

Combined effect of BaTiO<sub>3</sub> morphology and magnetoresistance or magnetostriction led to enhance the magneto-capacitance response of BaTiO<sub>3</sub>:ferrite composite systems.